Synergetic Control of the Mobile Self-Balanced Robot

Semen Podvalny
Voronezh State Technical University
Voronezh, Russia
spodvalny@yandex.ru

Eugeny Vasiljev
Voronezh State Technical University
Voronezh, Russia
vgtu-auts@yandex.ru

***Abstract*—This electronic document is a "live" template and alr *Abstract*—This article is devoted to an automatic motion control of the mobile self-balanced robot installed on a two-wheeled gyroscopic platform. The traditional solution of this task is to generate the control action for the engines of the wheels that would combine the stabilization process of horizontal position of the platform and its movement along the preset trajectory. Generally, when the frequency division or phase separation of these processes is impossible, then the position control and control of robot's motion interfere and exert the mutual perturbating effect. This influence is caused by kinematic and dynamic interrelations of coordinates of the mechanical system which is balancing freely on the mobile axis: any attempt to start movement or to deviate from the uniform rectilinear motion is accompanied inevitably with the deviation of the robot's longitudinal axis whereas any inclination of the platform leads to the emergence of the torques which move the platform on the surface of rolling. Any intention to suppress the internal interdependence of the coordinates of the system leads to further complication of control algorithms which requires considerable energy resources, viz., the overestimated power of engines and the capacities of storage batteries. To eliminate these fundamental shortcomings the synergetic approach is offered realizing the control of the considered system, i.e. to enter an additional minor operating influence – the position of the center of mass of a system. Working off this influence is carried out by the intrinsic kinematic and dynamic interrelations of the coordinates of a platform. As a result the system movement arises providing the matched solution for both the stabilization of the platform position and its coplanar motion. The two-member return pendulum kinematic scheme with the slowed-down hinge between the links was used for simulation and implementation of this control mode. The motion of the system's center of mass is realized in the form of angular deviation of the top link of a pendulum to the required angle. The mathematical model was built on the basis of the Lagrange's equations for kinetic energy of a system in the generalized coordinates in the form of two nonlinear differential equations of the second order. The center of masses position is entered to these equations in the form of a parameter. Indistinct regulators for each channel of regulation are synthesized and the operability test results of the offered automatic motion control are presented.**

Keywords—synergetic control, mobile robots, motion control of masses center

I. INTRODUCTION

Executive mechanisms installed on the bearing platform with two coaxial wheels or single spherical supports belong to the mobile self-balanced robots [1,2]. An advantage of this kinematic scheme of motion is robot's high maneuverability which is necessary for its movement in a limited space or in collaboration with several mobile mechanisms.

However, this specified advantage is inseparably linked with the robot's inherent drawback, i.e. the lack of instability in its vertical position [3]. In this regard any movement of a platform includes not only its linear motion on a plane surface but also the process of angular stabilization of robot's longitudinal axis in vertical position, i.e. the balancing. The joint implementation of motion and stabilization processes is carried out in most cases by one operating control action, namely, the control of the rotating moment of motors that are built in the wheels.

The analysis of physical content of this control method reveals its internal inconsistency, viz., any attempt of linear motion of a platform leads to robot balancing violation and an immediate counteraction aimed to restore vertical position, which reflects inevitably on the linear motion characteristics of a platform.

Such mutual influence of the specified processes is caused by the robot's own properties as an object of control. It is obvious that the coordinated control of these two processes is possible only when two channels of regulation are utilized in the system and, respectively, two control actions are realized to influence the process. In other words, the multidimensional control system must be created.

The practical embodiment of such system is possible on the basis of two approaches [4-7]:

to provide the regulation autonomy of robot's linear and angular coordinates;

to provide the connected regulation of these coordinates on the basis of synergetic approach to the control process, i.e. to use own internal coordinates interrelation of an object to achieve the control objective.

The synergetic control is understood in this case as the internally consistent, coordinated changes of these coordinates. The control of linear and angular coordinates of the robot developed by the system must work in strict accordance with physical interrelations between the specified coordinates, not despite of them [8-10]. Considerable simplification of control algorithms and deceleration of operating influences power shall be expected as a positive effect of such synergetic control.

The control problem on the basis of the first approach has been fully solved. This article is devoted to a less studied approach, namely, the synergetic approach to the control of a self-balanced robot.

II. SYNERGETIC CONTROL REALIZATION METHOD

To realize the synergetic control of the involved object the solution of a similar task for the "segway" mobile vehicle is offered to be used. The segway's control is exercised by the operator - the person standing directly on a platform, as shown in Fig. 1.

Let's single out the following stages of segway's interaction with the operator:

978-1-7281-6700-8/19/$31.00 ©2019 IEEE

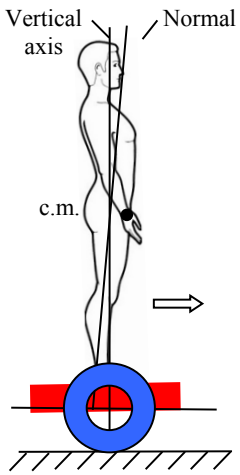

Fig. 1. Segway's control scheme (here, c.m. – is the center of masses)

- Initial motionless state. Longitudinal axes of a platform and the operator coincide and hold the vertical position. The mass center of the operator is not displaced relative to axis of the wheels.
- Motion start and speed setting. The operator displaces the masses center forward. The moment of gravity appears, under its influence the longitudinal axis of the operator begins to turn clockwise together with a platform, i.e. the balance is broken, see Fig. 1. The angular deviation of platform axis arising at the same time is sensed by gyroscopic sensors and the position stabilizing contour of the platform is activated. The motors of the wheels develop the moment restoring balance. At the same time, if this moment is sufficient to overcome the friction forces at rest, the wheels will start to rotate clockwise, and the platform will move to the right with constant acceleration.
- When the required preset speed is reached the operator restores the straight body position, not to the initial vertical position, but to make the moment of gravity equal to the moment of rolling friction. This position of masses center corresponds to the state of equilibrium in the system and to the uniform rectilinear motion of the stabilized platform.

The control process shown above fits the concept of synergetic control completely, i.e.:

1) it provides the decomposition of system to two control paths of upper and lower levels: the channel of motion of the masses center and the control path of wheels rotation;

2) the upper level control has low power and causes the motion of system provided exclusively with its own kinematic properties;

3) the coordination of the operating influences of both levels is not the result of the corresponding cross communications organization in the regulator, but as a result of the cross communications existence in the object of control.

Formal realization of the problem shown above can be formulated as follows: to find the off-line control $u_i(s) = R_i(s)\cdot\varepsilon_i(s)$, $i = 1,2$ of a multiply connected object $y(s) = W(s)\cdot u(s)+F(s)\cdot f(s)$ having the non-diagonal transfer matrix $W(s)$ with transfer matrixes $R_i(s)$.

The obtained control shall provide the resulting zero deviations $\varepsilon_i(s)$ of the controllable values $y_i(s)$ from the setting influences $g_i(s)$ in the presence of disturbances $f(s)$ imposed in the object according to a transfer matrix $F(s)$.

Let's now move on to to the described control process implementation and its subsequent numerical check using the imitating model.

III. Robot's Model as the Object of Control

A. Kinematic Scheme

The kinematic scheme of the robot is shown in Fig. 2 in the form of the inverted two-part pendulum, its parts (links) connected by the slowed-down hinge, shown in Fig. 2 [11,12].

The lower link 1 is connected to the wheels via a freely rotating axis. The rotating moments M_m of electric motors affects the corresponding wheels and simultaneously the link 1 in the opposite direction.

The angular deviation φ_2 of the link 2 from the a longitudinal axis of link 1 can be changed by way of mass center transfer of the link 2 forward or backward, imitating thereby the actions of the operator described in part II.

This system has two adjustable values: angular deviation φ_1 of a longitudinal axis from a vertical and the angle of wheels rotation ψ; two control influences: angular deviation φ_2 of link 2 from longitudinal axis of link 1, creating the rotating moment of gravity and the supply voltage of motors U (the rotating moment of motors). The revolting influence – is the moment M_{fk} of wheels rolling friction.

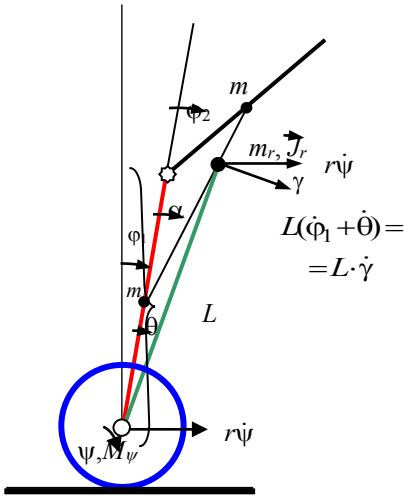

Fig. 2. Kinematic scheme of the robot as an object of control

B. Dynamic Model

To set up the motion equations of the described mechanical system the following parameters of its elements must be offered: m_1 and m_2 – the mass of links; L_1 and L_2 – distances of the mass centers m_1 to an axis of wheels and m_2 to the hinge; J_1 and J_2 – the moments of links inertia relative to the their masses centers; g – acceleration of

gravity; m – mass of a wheel; r – wheel radius; J – moment of wheel inertia; k_{fr} – friction coefficient of a wheel rolling; R – anchor winding resistance of the DC electric motor; C_e, C_m – constants on the back EMF and the moment of the motor.

The model of the obtained system was formed on the basis of Lagrange equations (1) for coordinates ψ and $\gamma = \varphi_1 + \theta$, , where θ – is the angle between the longitudinal axis of the robot and its calculated axis passing through the given mass center $m_r = m_1 + m_2$ and the axis of wheels rotation, as shown in Fig. 2:

$$\begin{aligned} \frac{d}{dt}\left(\frac{\partial T}{\partial \dot{\psi}}\right) - \frac{\partial T}{\partial \psi} &= M_\psi; \\ \frac{d}{dt}\left(\frac{\partial T}{\partial \dot{\gamma}}\right) - \frac{\partial T}{\partial \gamma} &= M_\gamma, \end{aligned} \tag{1}$$

where M_ψ and M_γ – the moments acting on the wheels and a platform, respectively; T – the kinetic energy of the system:

$$T = 2T_w + T_r \tag{2}$$

T_w and T_r – kinetic energy of the wheel and the platform, respectively:

$$T_w = \frac{J_w \cdot \dot{\psi}^2}{2} + \frac{m_w \cdot (r\dot{\psi})^2}{2}; \tag{3}$$

$$T_r = \frac{J_r(\dot{\phi}_1 + \dot{\theta})^2}{2} + \frac{m_r v_r^2}{2}, \tag{4}$$

v_r – absolute speed of the reduced masses center:

$$\begin{aligned} v_r^2 &= (r\dot{\psi})^2 + (L(\dot{\phi}_1 + \dot{\theta}))^2 + \\ &+ 2rL\dot{\psi}(\dot{\phi}_1 + \dot{\theta}) \cdot cos(\phi_1 + \theta). \end{aligned} \tag{5}$$

Substitution of (5) to (3),(4) and, hereafter of (3) and (4) to (2) gives the expression of total kinetic energy of the system:

$$\begin{aligned} T = &\left(m_w \cdot r^2 + J_w + \frac{m_r r^2}{2}\right) \cdot \dot{\psi}^2 + \\ &+ \left(\frac{m_r L^2 + J_r}{2}\right) \cdot \dot{\gamma}^2 + m_r rL\dot{\psi}\dot{\gamma} \cdot cos(\gamma), \end{aligned} \tag{6}$$

where J_r – the moment of inertia of the whole system concerning its masses center:

$$J_r = J_1 + J_2 + m_1 d^2 + m_2 (D - d)^2 \cdot \tag{7}$$

The J_r, L and γ values are the functions of the operating influence φ_2: $J_r(\varphi_2)$ $L(\varphi_2)$ and $\gamma(\varphi_2)$. Now we find the expressions for these functions.

In Fig. 2 we define the distance D between the concentrated mass m_1 and m_2:

$$D = \sqrt{L_1^2 + L_2^2 - 2L_1 L_2 \, cos(\pi - \phi_2)}, \tag{8}$$

distance d between the centers m_1 and m_r:

$$d = \frac{D \cdot m_2}{m_\kappa}, \tag{9}$$

length L of the reduced single-part pendulum and angle θ:

$$L = \sqrt{L_1^2 + d^2 - 2L_1 d \, cos(\pi - \alpha)}, \tag{10}$$

$$cos(\alpha) = \frac{L_1^2 + D^2 - L_2^2}{2L_1 D}. \tag{11}$$

Substituting (8), (9), (11) into (7), (10) and (12) we find $J_r(\varphi_2)$, $L(\varphi_2)$ and $\gamma(\varphi_2)$.

$$J_r(\phi_2) = \frac{\left(L_1^2 + L_2^2 + 2L_1 L_2 \, cos(\phi_2)\right) m_1 m_2}{m_r} + J_1 + J_2, \tag{13}$$

$$\begin{aligned} L(\phi_2) = &\left(2L_1 L_2 \frac{m_2}{m_r}\left(\frac{m_2}{m_r} + 1\right) cos(\phi_2) + \right. \\ &\left. + L_1^2 + \left(L_1^2 + L_2^2\right)\frac{m_2^2}{m_r^2} + 2\frac{m_2}{m_r} L_1^2\right)^{\frac{1}{2}}, \end{aligned} \tag{14}$$

$$\theta(\phi_2) = a\cos\left(\frac{L_1^2 + \frac{m_2}{m_r}\left(L_1^2 + L_1 L_2 \, cos(\phi_2)\right)}{L_1 L(\phi_2)}\right). \tag{15}$$

Moments M_ψ and M_γ in the right part of (1) are defined by the expressions:

$$M_\psi = 2M_m - (m_r + 2m_w) g k_{fr} \cdot sign(\dot{\psi}); \tag{16}$$

$$M_\gamma = m_r g L \cdot sin(\gamma) - 2M_m, \tag{17}$$

where

$$M_m = \frac{U - C_e(\dot{\psi} - \dot{\phi}_1)}{R} \cdot C_m. \tag{18}$$

Let's calculate the components (1):

$$\begin{aligned} \frac{\partial T}{\partial \dot{\psi}} &= \left(2m_w \cdot r^2 + 2J_w + m_r r^2\right) \cdot \dot{\psi} + m_r rL\dot{\gamma} \cdot cos(\gamma); \\ \frac{d}{dt}\left(\frac{\partial T}{\partial \dot{\psi}}\right) &= \left(2m_w \cdot r^2 + 2J_w + m_r r^2\right) \cdot \ddot{\psi} + \\ &+ m_r rL(\ddot{\gamma} \cdot cos(\gamma) - \dot{\gamma}^2 \cdot sin(\gamma)); \end{aligned} \tag{19}$$

$$\frac{\partial T}{\partial \psi} = 0; \tag{20}$$

$$\frac{\partial T}{\partial \dot{\gamma}} = \left(m_r l^2 + J_r\right)\cdot\dot{\gamma} + m_r rL\dot{\psi}\cdot cos(\gamma);$$
$$\frac{d}{dt}\left(\frac{\partial T}{\partial \dot{\gamma}}\right) = \left(m_r l^2 + J_r\right)\cdot\ddot{\gamma} + \tag{21}$$
$$+m_r rL(\ddot{\psi}\cdot cos(\gamma) - \dot{\psi}\dot{\gamma}\cdot sin(\gamma));$$

$$\frac{\partial T}{\partial \gamma} = -m_r rL\dot{\psi}\dot{\gamma}\cdot sin(\gamma). \tag{22}$$

After substitution of (16)-(22) into (1) we receive the required dynamic model of the robot:

$$\left(m_r L^2 + J_r\right)\cdot\ddot{\gamma} + m_r rL\cdot cos(\gamma)\cdot\ddot{\psi} =$$
$$= m_r gL\cdot sin(\gamma) - 2\frac{U - C_e(\dot{\psi} - \dot{\phi}_1)}{R}\cdot C_m; \tag{23}$$

$$\left(2m_w\cdot r^2 + 2J_w + m_r r^2\right)\cdot\ddot{\psi} + m_r rL(\ddot{\gamma}\cdot cos(\gamma) -$$
$$-\dot{\gamma}^2\cdot sin(\gamma)) = 2\frac{U - C_e(\dot{\psi} - \dot{\phi}_1)}{R}\cdot C_m - \tag{24}$$
$$-(m_r + 2m_w)g\cdot k_{fr}\cdot sign(\dot{\psi}).$$

The received model contains two nonlinear differential equations of the second order of rather adjustable coordinates ψ and $\varphi_1 = \gamma - \theta$. Voltage U and angle φ_2 are included into the equations as external influencing controls.

C. Check of Model Adequacy

Check of model adequacy (23), (24) was made using the MatLab mathematical package for two motion modes. In Fig. 3a the start of platform motion with constant angular deviation $\varphi_2 = 10.6$ deg ($\approx$0.184 rad) of the upper link 2 relative to the lower link 1 is shown. At the same time the platform loses balance, and its position tends to steady, but non-working value $\varphi_1 = \pi$ rad. If at the moment $t = 1.5$ s (Fig. 3b) φ_2 is reduced insignificantly (approximately to 0.183 rad), the platform continues the motion without balance loss.

Thus, the model adequately reproduces the physical features of the robot's motion shown above.

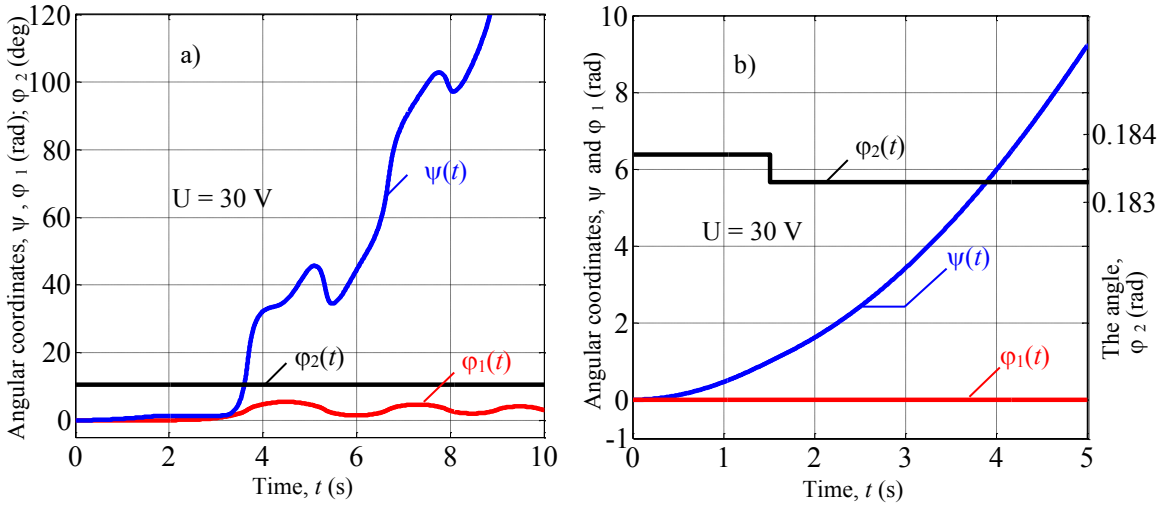

Fig. 3. Results of model adequacy check: a) the motion with a constant inclination $\varphi_2 = \text{const}$; b) the motion with the variable value φ_2 reduced at the timepoint $t = 1.5$ s.

IV. Control System

A. System Structure

The substantial analysis of the chosen way of robot's control provided in the section II indicates the need to implement two contours of regulation in the system:

a contour of linear movement regulation, or the angular speed $\dot{\psi}$ of wheels rotation; and the stabilizing contour of angular position of the robot longitudinal axis, i.e. its deviation φ_1 from a vertical, as shown in Fig. 4.

Whereas the stabilizing contour does not allow an emergence of fluctuations in the platform position, then, with the purpose of possible fluctuations damping we introduce the speed $\dot{\varphi}_1$ as the derivative of coordinate φ_1 into this contour. Moreover, considering the anthropogenous source of the synergetic control algorithm described above and the essential nonlinearity of the system (see model (23), (24)), we use the fuzzy regulators that are well adapted for control of nonlinear objects in the system.

Besides the transferred nodes, Fig. 4 shows the executive mechanism in the form of the quick-response linear motor moving the «operating» load with small weight, and the correcting link containing the integrator for providing the astatism of a regulation contour φ_1.

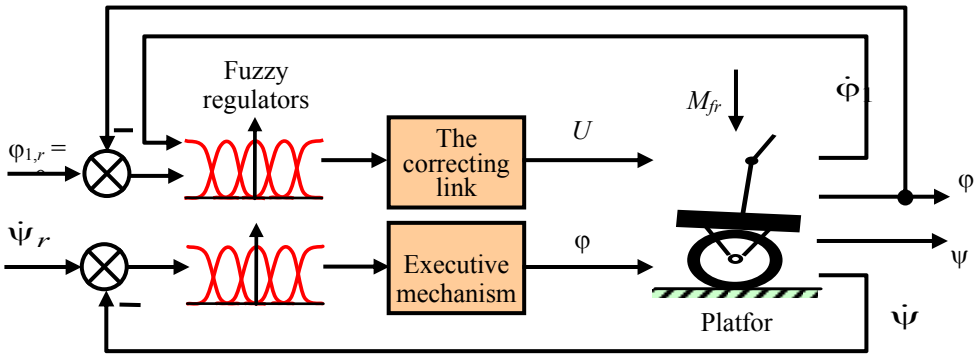

Fig. 4. General structure of a control system

B. Regulators

The fuzzy regulator of the stabilizing contour uses the linguistic variables $\alpha = \widetilde{\varphi}_1$ and $\beta = \widetilde{\dot{\varphi}}_1$ with five corresponding values:

$$\alpha = \{\alpha_1, \alpha_2, \alpha_3, \alpha_4, \alpha_5\}, \quad (25)$$

$$\beta = \{\beta_1, \beta_2, \beta_3, \beta_4, \beta_5\}, \quad (26)$$

for example: α_1 – a deviation of the platform angular position from a vertical which is both negative and considerably big; α_3 – the deviation is close to zero; α_5 – considerable positive deviation. Utilized accessory functions $\mu_{\alpha 1}(\varphi_1),\ldots, \mu_{\alpha 5}(\varphi_1)$ are shown in Fig. 5. The output linguistic variable $\gamma = \widetilde{U}$ contains five values either:

$$\gamma = \{\gamma_1, \gamma_2, \gamma_3, \gamma_4, \gamma_5\}, \quad (27)$$

where γ_1 – is to reduce the supply voltage U essentially ; γ_3 – practically should not be changed, etc.

The decisive rules $\alpha_i \,\&\, \beta_i \rightarrow \gamma_i$ (i = 1,…,5) for the regulator of stabilizing contour analyzes 25 combinations of α and β values, the table 1 (the non-single single weight coefficients of γ_i value are specified in brackets):

TABLE I. FUZZY VALUES OF γ OUTPUT VALUE OF THE STABILIZING CONTOUR REGULATOR

Value of α	Value of β				
	β1	β2	β3	β4	β5
α1	γ1	γ1	γ1(0.1)	γ2	γ3
α2	γ1	γ1	γ2	γ3	γ4
α3	γ2	γ2	γ3	γ4	γ4
α4	γ2	γ3	γ4	γ5	γ5
α5	γ3	γ4	γ5(0.1)	γ5	γ5

The regulator of a linear motion contour is built in the same manner.

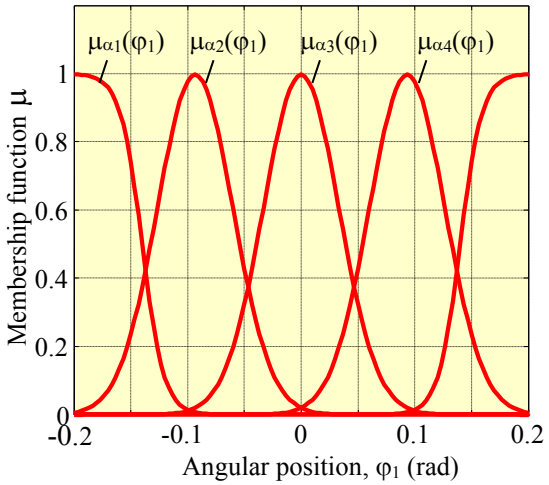

Fig. 5. Membership function μ of the regulator

C. System Operability Test

Operability of the offered control algorithm was tested for two operating system modes, viz., the mode of vertical position stabilization of the robot and the mode of acceleration to the preset speed of linear movement, as shown in Fig. 6.

Fig. 6a shows the process of placing the robot in vertical position at the initial inclination $\varphi_1(0) = 5$ deg: the platform starts moving quickly in the direction of the outlined falling and then it smoothly restores balance $\varphi_1 = 0$ deg, having moved forward f to a distance of 0.5 m or this purpose.

The acceleration of a platform (Fig. 6b) was provided by the initial deviation of an upper link to the angle $\varphi_2(0) = 17$ deg. The platform bends to 0.5 deg and accelerates gradually to the preset speed 0.26 m/s. At the same time vertical position of the platform is restored to $\varphi_1(6) \approx 0$ deg, whereas the tilt angle φ_2 tends to the value equal to approximately 6 deg, which is necessary for the creation of the gravity force moment which is equal to the rolling friction moment.

Thus, the system completely reproduces the preset control algorithms.

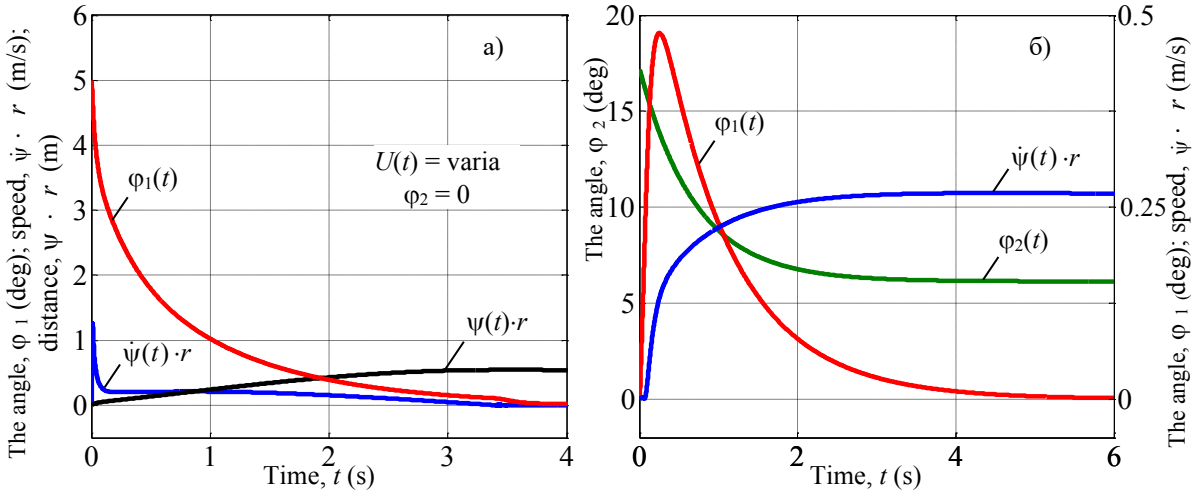

Fig. 6. System operability test in two modes: a) reduction to a vertical position at the initial deviation $\varphi_1(0) = 5$ deg; b) platform acceleration from the motionless state to 0.26 m/s linear speed

V. CONCLUSION

The offered way of synergetic approach implementation to solve the problem of self-balanced robot control by an additional motion of its masses center allows:

1) to exercise the related control of robot coordinates avoiding the formation of an artificial cross links in the regulator, but as a result of its own internal links use between these coordinates in the object;
2) to design independent autonomous regulators for each control path of the robot and, as a result, to simplify the algorithms of their functioning;
3) to use low-power executive mechanisms for the motion of the masses center, having excluded from this function the main drive of the wheels with built-in electric motors and reducing thereby the energy consumption from storage batteries.

REFERENCES

[1] M. Stilman, J. Olson, and W. Gloss, "Golem Krang: Dynamically Stable Humanoid Robot for Mobile Manipulation", Proceedings of the IEEE International Conference on Robotics and Automation, pp. 3304-3309, 2010.

[2] U. Nagarajan, G. A. Kantor, and R. Hollis, "Integrated Planning and Control for Graceful Navigation of Shape-Accelerated Underactuated Balancing Mobile Robots", Proceedings of the IEEE International Conference on Robotics and Automation, pp. 136-141, 2012.

[3] P. Kolhe, N. Dantam, and M. Stilman, "Dynamic Pushing Strategies for Dynamically Stable Mobile Manipulators", Proceedings. of the IEEE Int. Conf. on Robotics and Automation, pp. 3745-3750, 2010.

[4] K. Teeyapan, J. Wang, T. Kunz, and M. Stilman, "Robot Limbo: Optimized Planning and Control for Dynamically Stable Robots Under Vertical Obstacles", In IEEE International Conference on Robotics and Automation, Proceedings, ICRA'10, 2010.

[5] H. J. Yang, X. Z. Fan, P. Shi, and C. C. Hua, "Nonlinear Control for Tracking and Obstacle Avoidance of a Wheeled Mobile Robot With Nonholonomic Constraint", IEEE Transactions on Control Systems Technology, vol. 24, no. 2, pp. 741-746, 2016.

[6] F. Zacharias, C. Borst, M. Beetz, and G. Hirzinger, "Positioning Mobile Manipulators to Perform Constrained Linear Trajectories', In IEEE/RSJ International Conference on Intelligent Robots and Systems, IROS 2008, pp. 2578–2584, 2008.

[7] S. Roy, S. Nandy, R. Ray, and S. N. Shome, "Robust path tracking control of nonholonomic wheeled mobile robot: Experimental validation", International Journal of Control Automation & Systems, vol. 13, no. 4, pp. 897-905, 2015.

[8] S. L. Podvalny, and E.M. Vasiljev, "A Multi-alternative Approach to Control in Open Systems: Origins, Current State, and Future Prospects", Automation and Remote Control, vol. 76, no. 8, pp. 1471-1499, 2015.

[9] S.L. Podvalny, and E.M. Vasiljev, "Evolutionary principles for intellectual systems construction of multi-alternative control", Automation and Remote Control, vol. 76, no. 2, pp. 311-317, 2015.

[10] S.L. Podvalny, E.M. Vasiljev, and V.F. Barabanov, "Models of Multi-alternative Control and Decision-making in Complex Systems", Automation and Remote Control, vol. 75, no. 10, pp. 1886-1890, 2014

[11] R. Featherstone, "Analysis and Design of Planar Self-Balancing Double-Pendulum Robots. in Padois", Robot Design, Dynamics and Control, Springer, Vienna, pp. 259–266, 2013.

[12] V. H. Xinjilefu, V. Hayward and H. Michalska, "Stabilization of the Spatial Double Inverted Pendulum Using Stochastic Programming Seen as a Model of Standing Posture Control", Proc. 9th IEEE Int. Conf. Humanoid Robots, Paris, France, pp. 367–372, 2009.